

Nonlinear Impact Responses for a Damped Frame Supported by Nonlinear Springs with Hysteresis Using Fast FEA

T. Yamaguchi, M. Watanabe, M. Sasajima, C. Yuan, S. Maruyama, T. B. Ibrahim, H. Tomita

Abstract—This paper deals with nonlinear vibration analysis using finite element method for frame structures consisting of elastic and viscoelastic damping layers supported by multiple nonlinear concentrated springs with hysteresis damping. The frame is supported by four nonlinear concentrated springs near the four corners. The restoring forces of the springs have cubic non-linearity and linear component of the nonlinear springs has complex quantity to represent linear hysteresis damping. The damping layer of the frame structures has complex modulus of elasticity. Further, the discretized equations in physical coordinate are transformed into the nonlinear ordinary coupled differential equations using normal coordinate corresponding to linear natural modes. Comparing shares of strain energy of the elastic frame, the damping layer and the springs, we evaluate the influences of the damping couplings on the linear and nonlinear impact responses. We also investigate influences of damping changed by stiffness of the elastic frame on the nonlinear coupling in the damped impact responses.

Keywords—Dynamic response, Nonlinear impact response, Finite Element analysis, Numerical analysis.

I. INTRODUCTION

SPRINGS are often used not only for heavy structures but also for lightweight structures such as parts in automobiles to insulate them from external vibrations and shocks. However, in many cases, the stiffness of a lightweight structure is not sufficiently high for the structure to be considered rigid. Thus, in dynamic analysis, it is necessary to deal with these structures as elastic bodies. If the structures comprise resins, they should be treated as viscoelastic bodies.

Many researchers have studied for the nonlinear vibrations of concentrated masses with springs [1]. The authors previously proposed a fast numerical method to compute the nonlinear vibrations in an elastic/viscoelastic block with a nonlinear spring [2].

To reduce vibrations, viscoelastic damping materials are often laminated on the metal structures. Damping characteristics (e.g. modal loss factors) of these laminated panels are affected by not only properties of the viscoelastic

materials but also stiffness of the metal panels. To calculate the modal loss factors, which corresponds to modal damping when the structure are deformed as eigenmodes at resonant frequencies, complex eigenvalue analysis are often used. To compute the modal loss factors using FEM under linear problem, Johnson proposed Modal Strain Energy Method (i.e. MSE Method) [3], [4]. Using this method, the modal loss factors can be computed using material loss factor for each element and the ratio of modal strain energy for each element to total modal strain energy. This method is very useful to investigate damping mechanism in the metal structures with viscoelastic layers. However, there are few reports to treat nonlinear vibration problem of the metal structures with viscoelastic damping layers supported by nonlinear spring.

This paper describes vibration analysis using FEM for elastic structures with viscoelastic layers connected with nonlinear springs with hysteresis. We think this is a simplified model of a sub-frame supported by rubber mounts in automotive suspensions. The restoring force of the spring is expressed as power series of its deformation. A complex spring constant is introduced for the linear component of the restoring force. The finite elements for the nonlinear spring are expressed and they are attached to the elastic/ viscoelastic structures, which are modeled as solid finite elements with a complex modulus of elasticity. We obtain the nonlinear discrete equations of motion for the whole structure. To get modal loss factors, we introduce small parameters concerning damping to complex eigenvalue problem of the equations under small deformation. And we obtain asymptotic equations from the zero and first orders. Then, the approximate modal loss factors are obtained like MSE. Further, by introducing normal coordinate corresponding to eigenmodes. The nonlinear discrete equations in physical coordinates are transformed into nonlinear ordinary coupled equations. The transformed equations are rapidly computed to obtain the nonlinear transient responses with a fairly small dof.

As a numerical example of this proposed FEM, we deal with elastic frames with damping layers supported by multiple nonlinear springs with hysteresis. Using the proposed method, we show new phenomena including nonlinear coupling motions among nonlinear springs with hysteresis and elastic frames and viscoelastic layers. We clarify influences of amplitude of the impact force on nonlinear transient responses.

II. NUMERICAL MODEL

We use a simplified simulation model for frame structures supported by springs on four corners of the frame as shown in

T. Yamaguchi and S. Maruyama are with the Department of Mechanical System and Technology, Gunma University, Kiryu, Japan (e-mail: yamagme3@gunma-u.ac.jp).

M. Watanabe and M. Sasajima are with the Strategic Development Division, Foster electric Co.,Ltd., 196-8550, 1-1-109 Tsutsujigaoka, Akishima, Tokyo, Japan.

C. Yuan and T.B. Ibrahim are with the Graduate School of the Department of Mechanical System Engineering, Gunma University, Kiryu, Japan.

Fig. 1. We set the origin at one corner as shown in Fig. 1 in the $x-y$ plane on the upper surface of the frame. There exist four nonlinear springs in the z direction on each four corners. Further, on these corners, linear springs are set both in the x and y directions. The frame structures are composed of a steel frame and a viscoelastic damping layer. Fig. 2 shows three models which we investigate. The detail geometry of the models are shown in this figure. “Elastic Frame Model” as shown in Fig. 2 has only a steel frame. This has no viscoelastic damping layer. “Elastic Frame model with Damping Layer” has a steel frame with a damping layer. Thickness of the frame is 10mm and the thickness of the damping layer is 20mm. “High Stiffness Elastic Frame model with Damping Layer” has also a steel frame and a damping layer. But, thickness of the steel frame is 20mm which is twice of the thickness for “Elastic Frame model with Damping Layer”.

The concentrated nonlinear springs in the z direction have cubic nonlinearity in the relation between their displacement u_{mz} and their restoring force R_{mz} as shown in Fig. 3. Linear hysteresis damping is introduced into the restoring force of the nonlinear springs. Namely, linear components of the spring constants have complex quantity as $\gamma_{lm} = \bar{\gamma}_{lm}(1 + j\eta_s)$. η_s shows the loss factor of the springs. Further, there also exist linear concentrated springs in x and y directions at the corners. These linear springs have the same complex quantity as the linear component of the nonlinear springs. As shown in Fig. 1, the excitation point is $(x, y, z) = (575, 30, 0)$ on the upper surface of the steel frame. We evaluate impact responses of this simulation model. The evaluation point is $(x, y) = (575, 30)$ in Fig. 2 on the bottom surface of the frame with the damping layer.

III. NUMERICAL METHOD

We demonstrate a numerical method to calculate nonlinear responses by considering coupled damping properties for the elastic structures having viscoelastic damping layers connected to the nonlinear concentrated springs with linear hysteresis damping.

A. Discretized Equation for Nonlinear Concentrated Springs with Linear Hysteresis

First, we show discretized equations for the nonlinear concentrated springs with linear hysteresis [2]. We assumed that the nonlinear concentrated springs with viscoelasticity have the principal elastic axes in the z direction as illustrated in Fig. 1. We introduce the displacement as u_{mz} , ($m=1,2,3,\dots$) in the z direction at the nodal points α_m , ($m=1,2,3,\dots$) where the nonlinear springs are attached with the steel frame. The nodal force at the point α_m is expressed using the power series of u_{mz} . When cubic nonlinearity is assumed, the restoring force R_{mz} of the spring can be expressed as:

$$R_{mz} = \gamma_{1mz} u_{mz} + \gamma_{2mz} u_{mz}^2 + \gamma_{3mz} u_{mz}^3 \quad (1)$$

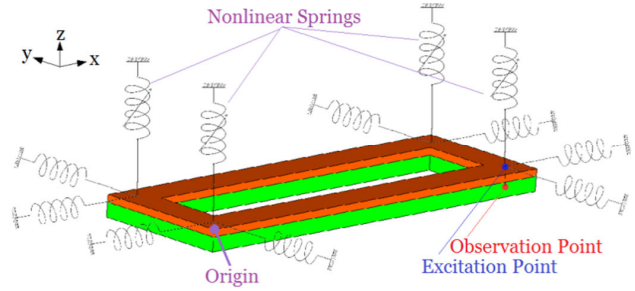


Fig. 1 Simulation model

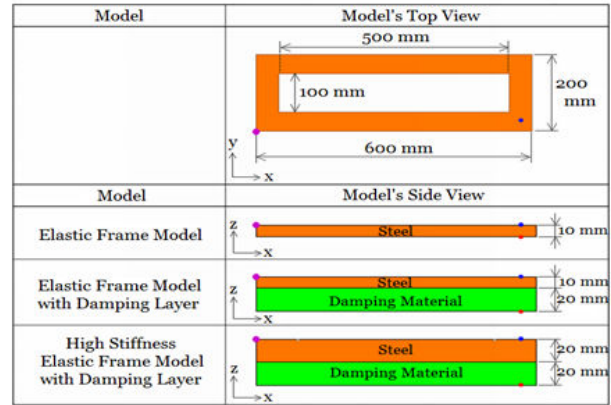


Fig. 2 Detail geometry of elastic frames with damping layer supported by nonlinear / linear springs

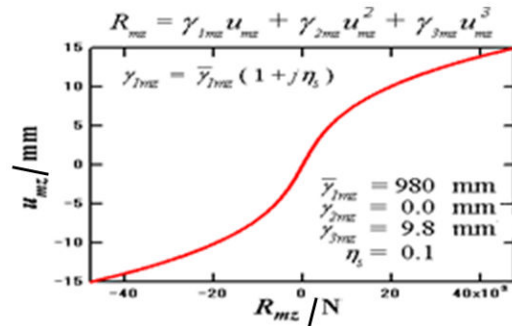


Fig. 3 Restoring force of nonlinear springs

Next, linear hysteresis damping is introduced as $\gamma_{lm} = \bar{\gamma}_{lm}(1 + j\eta_s)$. j is the imaginary unit. $\bar{\gamma}_{lm}$ is the real part of γ_{lm} , while η_s is the material loss factor of the spring. The relation in (1) can be rewritten in the matrix form as:

$$\{R_m\} = [\bar{\gamma}_{lm}] \{u_{sm}\} + \{\bar{a}_m\} \quad (2)$$

$$[\bar{\gamma}_{lm}] = \begin{bmatrix} 0 & 0 & 0 \\ 0 & 0 & 0 \\ 0 & 0 & \gamma_{1mz} \end{bmatrix}, \{\bar{a}_m\} = \{0, 0, \gamma_{2mz} u_{mz}^2 + \gamma_{3mz} u_{mz}^3\}^T \quad (3)$$

where $\{R_m\} = \{R_{mx}, R_{my}, R_{mz}\}^T$, $R_{mx} = R_{my} = 0$, is the nodal force

vector at the node $\alpha_m \cdot \{u_{sm}\} = \{u_{mx}, u_{my}, u_{mz}\}^T$ is the nodal displacement vector at the node α_m . $[\bar{y}_{lm}]$ is the complex stiffness matrix involving the linear term of the restoring force. $\{\bar{d}_m\}$ is the vector containing the nonlinear terms of the restoring force.

B. Discrete Equation for Elastic Frame and Viscoelastic Damping Material

For vibration of the steel frame and the viscoelastic damping material, we used discretized equations written in the following expressions from (4) and (5). They correspond to conventional linear finite element model in consideration of linear hysteresis damping. Stress-strain relation and strain-displacement relation are expressed as:

$$[M_s]_e \{\ddot{u}_s\}_e + [K_s]_e \{u_s\}_e = \{f_s\}_e \quad (4)$$

$[K_s]_e$ and $[M_s]_e$ are the element stiffness matrix and element mass matrix, respectively. $\{f_s\}_e$ and $\{u_s\}_e$ are the nodal force vector and nodal displacement vector in an element e .

By replacing complex modulus of elasticity with real modulus of elasticity, the viscoelastic damping layer can be modeled using finite elements. Consequently, the element stiffness matrix $[K_s]_e$ in (4) becomes to have complex quantities in (5):

$$[K_s]_e = [K_{sR}]_e (1 + j \eta_{se}) \quad (5)$$

$[K_{sR}]_e$ is the real part of element stiffness matrix for the viscoelastic damping material. η_{se} is the material loss factor corresponding to each element e .

For the elastic and the viscoelastic materials, isoparametric hexahedral elements with the non-conforming modes [5] are chosen. For the viscoelastic damping material, the storage modulus of elasticity is $8.00 \times 10^8 (\text{N/m}^2)$, the mass density is $1.45 \times 10^3 (\text{kg/m}^3)$ and the material loss factor η_{se} is 0.333.

C. Discrete Equations for Global System between the Nonlinear / Linear Springs and Damped Elastic Frame

The restoring force $\{R_m\}$ in (2) is added to the nodal force at the connected nodes α_m between the nonlinear concentrated springs in the z direction and the elastic frame. Further, the linear springs in the x and y directions are also attached. The next equation can be obtained for the global system [2]:

$$[M]\{\ddot{u}\} + [K]\{u\} + \{\hat{d}\} = \{f\}, \quad \{\hat{d}\} = \sum_{m=1} \{\hat{d}_m\} \quad (6)$$

where $\{f\}$, $[K]$, $[M]$, and $\{u\}$ are the external force vector, complex stiffness matrix, mass matrix, and displacement vector in the global system, respectively. $\{\hat{d}_m\}$ is modified from $\{\bar{d}_m\}$ to have a vector size identical to dof of the global system.

D. Computation of Modal Loss Factors

Next, we explain a computation method to obtain modal damping (i.e. modal loss factor) for the concentrated springs and the solid bodies (i.e. the elastic frame with the viscoelastic damping layer) in the global system. We neglect the nonlinear term under small deformation and the external force because of resonance conditions in (6). Next, it is assumed that $\{u\}$ can be expressed as $\{u\} = \{\phi\} e^{j\omega t}$. ω and t represent the angular frequency and the time, respectively. Consequently, we have homogeneous equation of (6), which corresponds to complex eigenvalue problem.

$$\sum_{e=1}^{e_{\max}} ([K_R]_e (1 + j\eta_e) - (\omega^{(i)})^2 (1 + j\eta_{tot}^{(i)}) [M_R]_e (1 + j\chi_e)) \{\phi^{(i)}\} = \{0\} \quad (7)$$

In this equation, η_e is the elements' material loss factors which includes η_s and η_{se} . $(\omega^{(i)})^2$ is the real part of complex eigenvalue. Superscript (i) stands for the i -th eigenmode. $\{\phi^{(i)}\}$ is the complex eigenvector. $\eta_{tot}^{(i)}$ is the modal loss factor. Next, we introduce the following β_{se} using the maximum value η_{\max} among the elements' material loss factors η_e , ($e=1, 2, 3, \dots, e_{\max}$).

$$\beta_{se} = \eta_e / \eta_{\max}, |\beta_{se}| \leq 1 \quad (8)$$

If we assume $|\eta_{\max}| \ll 1$, solutions (i.e. complex eigenvalues and complex eigenvectors) of (7) are expanded [4], [7] using a small parameter $\mu = j\eta_{\max}$:

$$\{\phi^{(i)}\} = \{\phi^{(i)}\}_0 + \mu \{\phi^{(i)}\}_1 + \mu^2 \{\phi^{(i)}\}_2 + \dots \quad (9)$$

$$(\omega^{(i)})^2 = (\omega_0^{(i)})^2 + \mu^2 (\omega_2^{(i)})^2 + \mu^4 (\omega_4^{(i)})^2 + \dots \quad (10)$$

$$j\eta_{tot}^{(i)} = \mu \eta_1^{(i)} + \mu^3 \eta_3^{(i)} + \mu^5 \eta_5^{(i)} + \mu^7 \eta_7^{(i)} + \dots \quad (11)$$

Under conditions of $\beta_{se} \leq 1$ and $|\eta_{\max}| \ll 1$, we can obtain $|\eta_{\max} \beta_{se}| \ll 1$. Thus, $\mu \beta_{se}$ can be regarded as small parameters like μ . In (9), (10) and (11), $\{\phi^{(i)}\}_0$, $\{\phi^{(i)}\}_1$, $\{\phi^{(i)}\}_2, \dots$ and $(\omega_0^{(i)})^2$, $(\omega_2^{(i)})^2$, $(\omega_4^{(i)})^2, \dots$ and $\eta_1^{(i)}$, $\eta_3^{(i)}$, $\eta_5^{(i)}, \dots$ have real quantities. By substitution of these expressions from (9) to (11) into (7), we obtain approximate equations using μ^0 and μ^1 orders. Finally, the following equation can be derived by arranging the approximate equations:

$$\eta_{tot}^{(i)} = \sum_{e=1}^{e_{\max}} (\eta_e S_{se}^{(i)}) \quad (12)$$

From (12), modal loss factor $\eta_{tot}^{(i)}$ can be calculated using material loss factors η_e of each element e and share $S_{se}^{(i)}$ of strain energy of each element to total strain energy. This

equation has the same form of MSE Method [3], [4] proposed by Johnson. This method helps us to decrease computational time for large-scale finite element models for the damped structure. And in (12), $\eta_e S_{se}^{(i)}$ corresponds to contribution of each element e to i -the modal damping. Using this, we can analyze coupled damping properties in the elastic frame with viscoelastic damping layer supported by complex springs having linear hysteresis.

E. Conversion to Nonlinear Equations in Normal Coordinate from Equation in Physical Coordinate

When we compute impact responses using (6) in physical coordinates directly, it takes considerable computational time. We adopt a numerical procedure to diminish the degree of freedom for the discretized equations of motion [2], [6].

We assume that the linear natural modes of vibration $\{\phi^{(i)}\}$ can be approximated to $\{\tilde{\phi}^{(i)}\}_0$. Further, the nodal displacement vector can be expressed by introducing normal coordinates \tilde{b}_i corresponding to the linear natural modes $\{\phi^{(i)}\}_0$ as:

$$\{u\} = \sum_{i=1} \tilde{b}_i \{\tilde{\phi}^{(i)}\}_0 / n_i \quad (13)$$

where

$$\{\phi^{(i)}\}_0 = \sqrt{m_i} \{\tilde{\phi}^{(i)}\}_0 = \{\tilde{\phi}^{(i)}\}_0 / n_i, n_i = 1 / \sqrt{m_i},$$

$$m_i = \{\phi^{(i)}\}_0^T [M] \{\phi^{(i)}\}_0, \{\tilde{\phi}^{(i)}\}_0^T [M] \{\tilde{\phi}^{(i)}\}_0 = 1$$

By substitution of (13) into (6), the following nonlinear ordinary simultaneous equations with regard to normal coordinates \tilde{b}_i can be obtained.

$$\ddot{\tilde{b}}_i + \eta_{tot}^{(i)} \omega^{(i)} \dot{\tilde{b}}_i + (\omega^{(i)})^2 \tilde{b}_i + \sum_j \tilde{D}_{ijk} \tilde{b}_j \tilde{b}_k + \sum_j \sum_k \sum_l \tilde{E}_{ijkl} \tilde{b}_j \tilde{b}_k \tilde{b}_l = \tilde{P}_i \quad (14)$$

$$\{\tilde{\phi}^{(i)}\}_0 = \{\tilde{\phi}_{i1x}, \tilde{\phi}_{i1y}, \tilde{\phi}_{i1z}, \tilde{\phi}_{i2x}, \tilde{\phi}_{i2y}, \tilde{\phi}_{i2z}, \tilde{\phi}_{i3x}, \dots\}^T,$$

$$\tilde{P}_i = n_i \{\tilde{\phi}^{(i)}\}_0^T \{F\}, \tilde{D}_{ijk} = \sum_{m=1}^4 \tilde{\gamma}_{2my} (n_i / (n_j n_k)) \tilde{\phi}_{imy} \tilde{\phi}_{jmy} \tilde{\phi}_{kmy}$$

$$\tilde{E}_{ijkl} = \sum_{m=1}^4 \tilde{\gamma}_{3my} (n_i / (n_j n_k n_l)) \tilde{\phi}_{imy} \tilde{\phi}_{jmy} \tilde{\phi}_{kmy} \tilde{\phi}_{lmy}$$

We can save computational time because (14) has a much smaller degree of freedom than (6). $\tilde{\phi}_{iimz}$ is the z -component of the eigenmode $\{\tilde{\phi}^{(i)}\}_0$ at the m -th connected node α_m between the frame and the nonlinear springs. The damping term in (14) can be derived in an identical form to (12).

IV. NUMERICAL RESULTS AND DISCUSSION

A. Results of and Modal Loss Factors and Eigenmodes and Resonant Frequencies

Figs. 4 and 5 show eigenmodes $\{\tilde{\phi}^{(i)}\}_0$, resonant frequencies $\omega_0^{(i)} / (2\pi)$ and modal loss factors $\eta_{tot}^{(i)}$ for modes 1 to 14 and modes 15 to 21, respectively.

In these figures, arrows stand for directions of rigid motions in eigenmodes especially.

We give the material loss factors of the steel frames as $\eta_e = \eta_f = 0.001$. And that of the viscoelastic damping layer is $\eta_e = \eta_d = 0.333$. Those of the springs are $\eta_e = \eta_s = 0.100$.

In these figures, results for the three models are shown. Results of “Elastic Frame Model” in Fig. 2 are the left deformation patterns in Figs. 1 and 2. Results of “Elastic Frame Model with Damping Layer” in Fig. 2 are the central deformation patterns. Results of “High Stiffness Elastic Frame Model with Damping Layer” in Fig. 2 are the right deformation patterns.

In this paper, material loss factor $\eta_s = 0.100$ of the springs are larger than $\eta_f = 0.001$ of the steel frame. If eigenmodes include no elastic deformation of the steel frame, the modal loss factors are close to $\eta_s = 0.100$. Thus, modal loss factor $\eta_{tot} = 0.996$ of mode 4 (i.e. rigid mode of the frame) is larger than $\eta_{tot} = 0.0014$ for mode 13 (i.e. elastic mode of the steel frame). Because the deformation of the springs is dominant in mode 4, the share of the strain energy in (12) in the springs is large. This leads to high modal loss factor. On the other hand, the deformation of the springs is small in modes from 10 to 20 due to the elastic mode of the steel frame without damping layer. This leads to low modal loss factor.

For mode 2 including both rotation of the steel frame about the x axis and elastic deformation of the frame, the modal loss factor $\eta_{tot} = 0.0564$ is middle value between those for modes 4 and 13. These phenomena are generated due to dependence of eigenmodes on the share of the strain energy in (12).

Modal loss factor η_{tot} of mode 10 for “Elastic Frame Model with Damping Layer” is larger than that of mode 10 for “Elastic frame Model”. Because the viscoelastic damping material has high material loss factor $\eta_d = 0.333$, modal loss factors η_{tot} for modes from 10 to 20 including elastic deformation of the frame increase.

If we assume to remove the springs, we set that modal loss factors η_{tot} of the laminate (i.e. 10mm thickness of the steel frame plus 10mm thickness of the damping layer) are less than the material loss factor $\eta_s = 0.100$ of the springs. Therefore $\eta_{tot} = 0.997$ of mode 4 including larger deformations in the springs is larger than $\eta_{tot} = 0.0467$ of mode 13 including larger elastic deformation in the steel frame. Modal loss factor $\eta_{tot} = 0.0564$ of mode 2 shows a middle value between them (i.e. modes 4 and 13) because this mode contains both elastic deformation in

the steel frame and the deformation in springs when rotating motions of the frame occur.






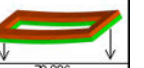


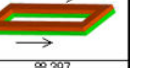

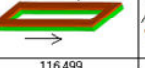

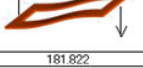
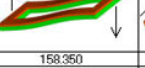
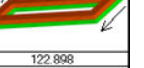

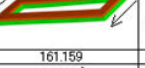
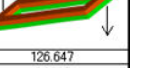



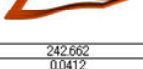
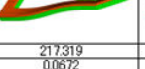
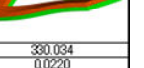
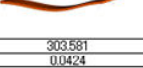
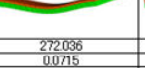
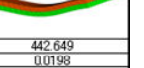


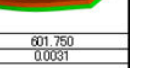
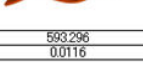
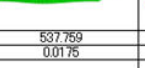
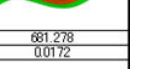
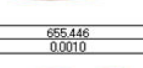
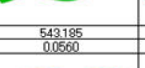
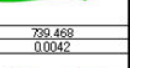
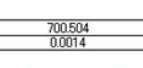
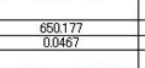
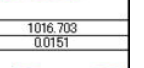
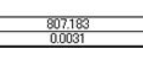
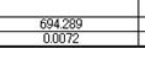
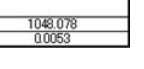
Vibration Mode	Elastic	Elastic with Damping Layer	High Stiffness Elastic with Damping Layer
1			
Frequency [Hz]	70.309	65.346	78.086
Modal Loss Factor	0.0214	0.0722	0.0964
2			
Frequency [Hz]	103.096	90.813	79.086
Modal Loss Factor	0.0564 *	0.082 *	0.0813 *
3			
Frequency [Hz]	134.924	116.144	88.397
Modal Loss Factor	0.0971 *	0.0966 *	0.0998
4			
Frequency [Hz]	135.910	116.499	93.775
Modal Loss Factor	0.0996	0.0997	0.0963
5			
Frequency [Hz]	181.822	158.350	122.898
Modal Loss Factor	0.0828 *	0.0945 *	0.0994
6			
Frequency [Hz]	188.555	161.159	126.647
Modal Loss Factor	0.099 *	0.0988 *	0.0985
7			
Frequency [Hz]	241.390	211.710	264.202
Modal Loss Factor	0.0777	0.0901	0.0361
8			
Frequency [Hz]	242.662	217.319	380.034
Modal Loss Factor	0.0412	0.0672	0.0220
9			
Frequency [Hz]	303.581	272.036	442.649
Modal Loss Factor	0.0424	0.0715	0.0198
10			
Frequency [Hz]	391.082	362.817	601.750
Modal Loss Factor	0.0172	0.0658	0.0031
11			
Frequency [Hz]	593.296	537.759	681.278
Modal Loss Factor	0.0116	0.0175	0.0172
12			
Frequency [Hz]	655.446	543.185	739.468
Modal Loss Factor	0.0010	0.0560	0.0042
13			
Frequency [Hz]	700.504	650.177	1016.703
Modal Loss Factor	0.0014	0.0467	0.0151
14			
Frequency [Hz]	807.183	694.289	1048.078
Modal Loss Factor	0.0031	0.0072	0.0053

Fig. 4 Vibration modes for mode 1 to mode 14

















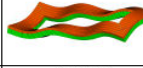
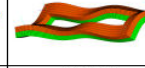
Vibration Mode	Elastic	Elastic with Damping Layer	High Stiffness Elastic with Damping Layer
15			
Frequency [Hz]	825.121	735.879	1196.660
Modal Loss Factor	0.0026	0.0511	0.0159
16			
Frequency [Hz]	956.608	836.983	1384.911
Modal Loss Factor	0.0023	0.0422	0.0166
17			
Frequency [Hz]	1126.364	928.771	1569.649
Modal Loss Factor	0.0024	0.0391	0.0153
18			
Frequency [Hz]	1148.874	1031.193	1633.472
Modal Loss Factor	0.0011	0.0531	0.0095
19			
Frequency [Hz]	1148.976	1038.075	1811.926
Modal Loss Factor	0.0028	0.0192	0.0160
20			
Frequency [Hz]	1375.819	1208.082	2009.518
Modal Loss Factor	0.0019	0.0548	0.0164

Fig. 5 Vibration modes for mode 15 to mode 20

Because thickness of the steel frame for this model is 20mm, which is double for “Elastic Frame Model with Damping Layer”, this frame has higher stiffness. However, due to this high rigidity, damping decreases for modes from 10 to 20 having large deformation in the frame. For instance, modal loss factor $\eta_{tot} = 0.0166$ of this model for mode 16 is less than $\eta_{tot} = 0.0511$ of “Elastic Frame Model with Damping Layer” for mode 15. According to (12), not only material loss factors but also share of strain energy is required to increase modal loss factors. Therefore, to increase modal loss factors of the frame with the damping layer, high share of the strain energy in the viscoelastic damping layer is required. Actually, we can find lower share of strain energy of the steel frame for “Elastic Frame Model with Damping Layer” as shown in Fig. 7 than that for “High Stiffness Elastic Frame Model with Damping Layer” as shown in Fig. 6. Using the proposed method, this phenomenon can be also explained roughly by Oberst expression [8] from theoretical analysis using complex flexural rigidity for bending vibrations of a beam having a non-constraint type viscoelastic damping layer. Damping becomes low when neutral plane of the frame with viscoelastic layer is apart from the damping layer.

As we mentioned before, this model has the thick frame. Due to high stiffness of the frame, elastic deformations of the steel frame become very small in modes 1 to 6, which we can almost regard as rigid motions for the frame. This leads that modal loss factors for these modes are close to the value of the material loss factor $\eta_s = 0.100$ of the springs.

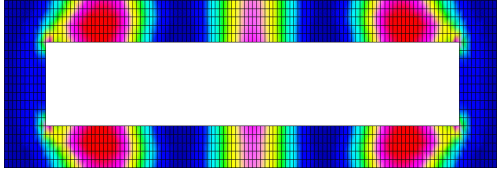


Fig. 6 Strain energy distribution in steel frame for "High Stiffness Elastic Frame Model with Damping Layer"(Mode 16)

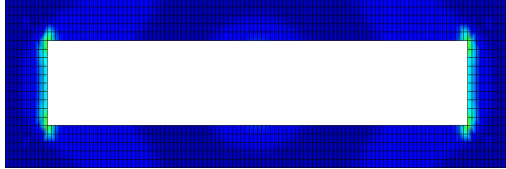


Fig. 7 Strain energy distribution in steel frame for "Elastic Frame Model with Damping Layer"(Mode 15)

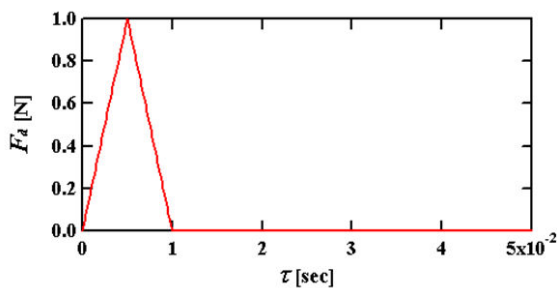


Fig. 8 Time history of impact force

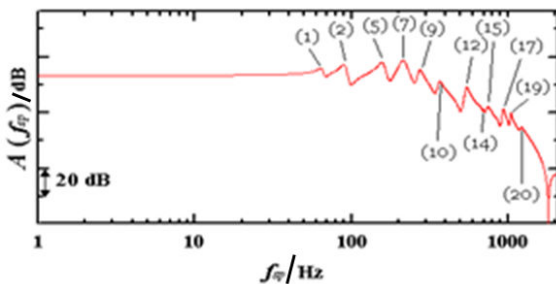


Fig. 9 Fourier spectrum of impact response for "Elastic Frame Model" under small input ($|f_{\max}| = 0.98 \text{ N}$)

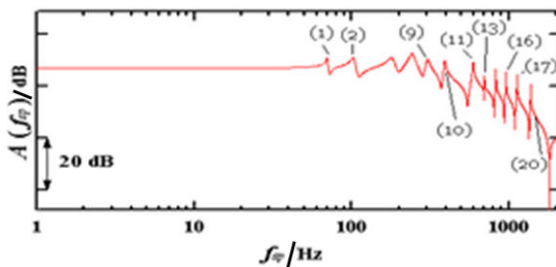


Fig. 10 Fourier spectrum of impact response for "Elastic Frame Model" under large input ($|f_{\max}| = 9.8 \times 10^5 \text{ N}$)

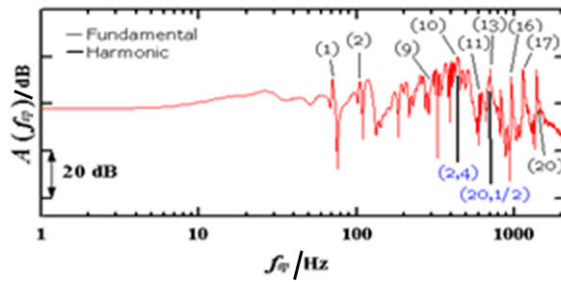


Fig. 11 Fourier spectrum of impact response for "Elastic Frame Model with Damping Layer" under small input ($|f_{\max}| = 0.98 \text{ N}$)

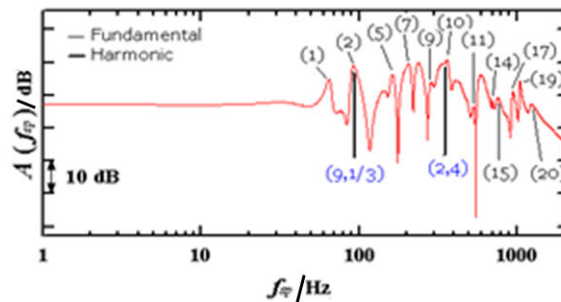


Fig. 12 Fourier spectrum of impact response for "Elastic Frame Model with Damping Layer" under large input ($|f_{\max}| = 9.8 \times 10^5 \text{ N}$)

A. Results of Impact Responses

By changing the maximum amplitude $|f_{\max}|$ of the impact as shown in Fig. 8 under a constant pulse width 0.001 (s), transient time histories are computed. In Fig. 8, the ordinate F_d represents force amplitude, while the abscissa τ shows time. And we evaluate displacement at the evaluation point on the frame as shown in Fig. 1.

In Figs. 9 and 10, the ordinate represents amplitude of frequency response function $A(f_{sp})$, while the abscissa shows Fourier frequency f_{sp} . As for (m) in Fig. 9, m denotes m -th vibration mode. For (m, n) in Fig. 10, m denotes m -th vibration mode and n denotes types of the frequency response function. For instance, $n=3$ shows super-harmonic component of the third order and $n=1/2$ represents sub-harmonic component of the 1/2 order. 0 (dB) represents the amplitude of the spectrum equals 1(mm) for $A(f_{sp})$ in these figures. Fig. 9 represents the frequency response function of a time history under the small impact force $|f_{\max}| = 0.98 \text{ (N)}$. And Fig. 10 shows the frequency response function of the time history under the extraordinary large impact force $|f_{\max}| = 9.8 \times$

Under the small input force $|f_{\max}| = 0.98 \text{ (N)}$ in Fig. 9, the peaks of the modes 1,2,5,7,9, 10,11,13,15,16,17 and 20 appear in the frequency response function mainly. Because excitation force in the z direction is acted on and the direction of observation is z , these modes include large amplitudes in the z direction.

Due to small modal loss factors including large elastic deformations in the steel frame and small deformation in the springs with linear hysteresis, the peaks for modes from 10 to 20 show sharp and have large amplitudes.

Under the extraordinary large input force $|f_{\max}| = 9.8 \times 10^5 \text{ (N)}$ in Fig. 10, there exist many peaks (i.e. not only fundamental components but also super harmonic, sub-harmonic components and internal resonances) for modes including large deformation in the nonlinear springs in the frequency response function.

We investigate linear and nonlinear transient responses for “Elastic Frame Model with Damping Layer”. Fig. 11 represents the frequency response function of a time history under the small impact force $|f_{\max}| = 0.98 \text{ (N)}$. Fig. 12 shows the frequency response function under the extraordinary large impact force $|f_{\max}| = 9.8 \times 10^5 \text{ (N)}$.

Under the small input force $|f_{\max}| = 0.98 \text{ (N)}$ in Fig. 11, the peaks of the modes 1,2,5,7,9, 10,11,13,15,16,17 and 20 appear in the frequency response function like Fig. 9 for the model without damping layer. However, the amplitudes decrease for the peaks for modes from 10 to 20 including large deformations in the frame with damping layer. On the other hand, in comparison with Fig. 9, there exist small changes in the peaks for modes 3, 4 and 6 including large deformation in the springs and small deformations in the frame.

Under the extraordinary large input force $|f_{\max}| = 9.8 \times 10^5 \text{ (N)}$ in Fig. 12, in comparison with Fig. 10 for the model without damping layer, number of the nonlinear peaks decrease. Especially, due to higher damping, this phenomenon is outstanding for modes from 10 to 20 including large deformation in the frame with the damping layer. Therefore, the damping layer enables us to diminish the nonlinear coupling in the transient response.

Next, we investigate the transient responses for “High Stiffness Elastic Frame Model with Damping Layer” and clarify influences of the stiffness of the steel frame on linear / nonlinear transient responses. As we stated previously in previous section A, modal loss factors of this model decrease due to high stiffness of the steel frame for modes 10 to 20 containing large deformations in the frame with the damping layer. Fig. 13 represents the frequency response function of a time history under the small impact force $|f_{\max}| = 0.98 \text{ (N)}$. Fig. 14 shows the frequency response function of a time history under the extraordinary large impact force $|f_{\max}| = 9.8 \times 10^5 \text{ (N)}$.

Under the small input force $|f_{\max}| = 0.98 \text{ (N)}$ in Fig. 13, the peaks of the modes 1,2,4,6,7, 9,11,13,16 and 18 appear in the frequency response function like Fig. 11 for “Elastic Frame Model with Damping Layer”. Nevertheless, the amplitudes increase for the peaks for modes from 10 to 20 including large deformations in the frame with damping layer. This phenomenon is caused by low modal loss factors of these modes due to high stiffness of the steel frame as we explained in previous Section A.

Under the extraordinary large input force $|f_{\max}| = 9.8 \times 10^5 \text{ (N)}$ in Fig. 14, in comparison with Fig. 12 for the model without damping layer, number of the nonlinear peaks increase. Especially, due to lower damping oriented from high stiffness of the steel frame, this phenomenon is notable for modes from 10 to 20 including large deformation in the frame with the damping layer. Therefore, if we increase the thickness of the steel frame, damping of the frame with the damping layer diminishes and this leads to magnify the nonlinear coupling in the transient response, consequently.

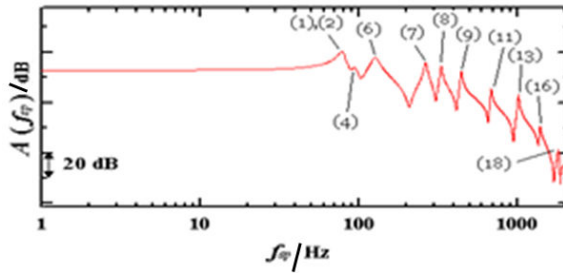


Fig. 13 Fourier spectrum of impact response for “High Stiffness Elastic Frame Model with Damping Layer” under small input ($|f_{\max}| = 0.98 \text{ N}$)

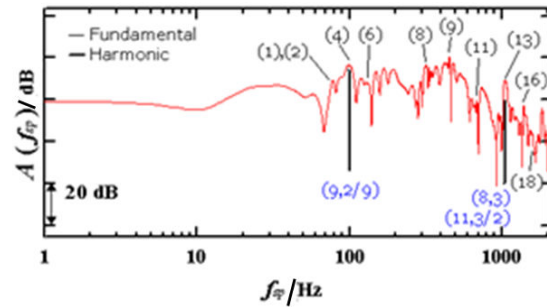


Fig. 14 Fourier spectrum of impact response for “High Stiffness Elastic Frame Model with Damping Layer” under large input ($|f_{\max}| = 9.8 \times 10^5 \text{ N}$)

V. CONCLUSION

This paper describes vibration analysis using FEM for elastic frames with viscoelastic layers connected with multiple nonlinear springs with hysteresis. The restoring force of the spring is expressed as power series of its elongation. A complex spring constant is introduced for the linear component of the restoring force. The finite elements for the nonlinear spring are expressed and they are attached to the elastic/ viscoelastic structures, which are modeled as solid finite elements with a complex modulus of elasticity. To get modal loss factors, we introduce small parameters concerning damping to complex eigenvalue problem of the equations under small deformation. And we obtain asymptotic equations from the zero and first orders. Then, the approximate modal loss factors are obtained like MSE. Further, by introducing normal coordinate corresponding to eigenmodes. The nonlinear discrete equations

in physical coordinates are transformed into nonlinear ordinary coupled equations.

We show phenomena including nonlinear coupled damped motions between nonlinear springs with hysteresis and elastic frames and viscoelastic layers by increasing impact force. Under a very large impact force as a severe condition, there exist complicated nonlinear couplings in Fourier spectrum. Due to high damping oriented from viscoelastic damping layer, nonlinear peaks are diminished. When we increase thickness of the steel frame, damping of the frame with the viscoelastic layer decreases. This causes the spectrum of the transient response includes more peaks due to nonlinear couplings.

ACKNOWLEDGMENT

This work was supported by JSPS KAKENHI Grant Number 26420167.

We used a software named as HyperMesh v11.0 (Altair Engineering Inc.) to create simulation models in this paper.

REFERENCES

- [1] E. Pesheck, N. Boivin, C. Pierre and S. W. Shaw, "Non-linear modal analysis of structural systems using multi-mode invariant manifolds", *Nonlinear Dynamics*, Vol.25, pp.183-205, 2001.
- [2] T. Yamaguchi, Y. Fujii, K. Nagai and S. Maruyama, "FEM for vibrated structures with non-linear concentrated spring having hysteresis", *Mechanical Systems and Signal Processing*, Vol.20, pp.1905-1922, 2006.
- [3] C. D. Johnson and D. A. Kienholz, "Finite element prediction of damping structures with constrained viscoelastic layers", *AIAA Journal*, Vol.20, No.9, pp.1284-1290, 1982.
- [4] B. A. Ma and J. F. He, "A finite element analysis of viscoelastically damped sandwich plates", *Journal of Sound and Vibration* Vol.152, No.1, pp.107-123.
- [5] O. C. Zienkiewicz and Y. K. Cheung, *The finite element method in structural and continuum mechanics*, MacGraw-Hill, 1967.
- [6] T. Yamaguchi and K. Nagai, "Chaotic vibration of a cylindrical shell-panel with an in-plane elastic support at boundary", *Nonlinear Dynamics*, Vol.13, pp.259-277, 1997.
- [7] T. Yamaguchi, Y. Kurosawa and H. Enomoto, "Damped vibration analysis using finite element method with approximated modal damping for automotive double walls with a porous material", *Journal of Sound and Vibration*, Vol.325, pp.436-450, 2009.
- [8] H. Oberst, *Akustische Beihefte*, Vol.4, pp.181-194, 1952.